

Research Article

Effect of RGD Peptide-Coated TiO₂ Nanotubes on the Attachment, Proliferation, and Functionality of Bone-Related Cells

Seunghan Oh,¹ Kyung Suk Moon,¹ and Seoung Hoon Lee²

¹ Department of Dental Biomaterials and Institute of Biomaterials-Implant, College of Dentistry, Wonkwang University, Jeonbuk, Iksan 570-749, Republic of Korea

² Department of Oral Microbiology and Immunology, College of Dentistry, Wonkwang University, Jeonbuk, Iksan 570-749, Republic of Korea

Correspondence should be addressed to Seunghan Oh; shoh@wku.ac.kr and Seoung Hoon Lee; leesh2@wku.ac.kr

Received 4 June 2013; Revised 12 July 2013; Accepted 12 July 2013

Academic Editor: Jiamin Wu

Copyright © 2013 Seunghan Oh et al. This is an open access article distributed under the Creative Commons Attribution License, which permits unrestricted use, distribution, and reproduction in any medium, provided the original work is properly cited.

The purpose of this research was to characterize an Arg-Gly-Asp (RGD) peptide immobilized on TiO₂ nanotubes. In addition, we investigated the effects of the RGD peptide-coated TiO₂ nanotubes on the cellular response, proliferation, and functionality of osteogenic-induced human mesenchymal stem cells (hMSCs), which are osteoclasts that have been induced by bone marrow macrophages. The RGD peptide was grafted covalently onto the surface of TiO₂ nanotubes based on the results of SEM, FT-IR, and XPS. Furthermore, the RGD peptide promoted the initial attachment and proliferation of the hMSCs, regardless of the size of the TiO₂ nanotubes. However, the RGD peptide did not prominently affect the osteogenic functionality of the hMSCs because the peptide suppressed hMSC motility associated with osteogenic differentiation. The result of an *in vitro* osteoclast test showed that the RGD peptide accelerated the initial attachment of preosteoclasts and the formation of mature osteoclasts, which could resorb the bone matrix. Therefore, we believe that an RGD coating on TiO₂ nanotubes synthesized on Ti implants might not offer significant acceleration of bone formation *in vivo* because osteoblasts and osteoclasts reside in the same compartment.

1. Introduction

The clinical success and long-term stability of implants are determined by osseointegration between implantation materials and bone tissue [1]. Several studies exploring various surface treatments of the Ti implants have been conducted because of the excellent amenability to surface coating, which can promote successful bonding between bone tissue and implants and reduce the implantation healing period [1, 2]. To overcome the limitation of current osseointegration of implants and to enhance the tissue response *in vivo*, recent developments in implant surface treatments have focused on optimizing the interfacial reaction between the implant and the surrounding bone tissue on the basis of the chemical properties, charge, microstructure, and porosity of the implant surfaces [1–4].

Various chemical and physical methods such as chemical oxidation, plasma oxidation, and electrochemical anodization techniques have been adopted to prepare a biologically feasible oxide layer on a Ti surface [5]. Among them, anodization of the Ti surface has the potential to increase the porosity of the Ti surface and improve the surface area to promote cell attachment [6–8].

Nanostructures, including TiO₂ nanotubes, have recently been the focus of great interest for biological and biomedical applications owing to their high surface-to-volume ratio and higher structural plasticity compared to that of microscale structures. In terms of biomaterial development and implant technology, cellular responses can be affected by topographical circumstances. It is well known that variability in cell responses due to nanostructural topography *in vitro* alters cell morphology, cytoskeletal structure, gene expression, and

so forth [9–15]. Nanosized topographical factors have been shown to affect cells and tissues *in vivo* as well [8, 16–19]. In addition, a nanotopographical factor plays a critical role in improving the rate of cell proliferation and tissue acceptance, thereby ultimately determining the usefulness of the implanted biomaterial.

Recently, many studies using biochemical materials such as the extracellular matrix (ECM), growth factors, and bioactive materials as surface coating have been conducted to achieve osteoinduction and osteoconduction together. Osteoconduction is the growth of bones on the surface of the implant, and it relates to the biocompatibility of the implant materials. Osteoinduction is the phenomenon whereby osteogenesis is induced, and it is supposed to be a bone-healing process as it recruits immature cells and stimulates the cells into becoming osteoblasts [20]. Therefore, to achieve excellent osseointegration, osteoconduction and osteoinduction can be determined from the characteristics of the biochemical materials used, and materials that promote osteogenesis among immature cells in the body can be selected [21].

The Arg-Gly-Asp (RGD) peptide is a prospective bioactive factor and an amino acid present in integrin. The RGD peptide also regulates the attachment of cell proteins and the ECM. This peptide mediates the bonds between cellular, plasma, and ECM proteins, such as fibronectin, vitronectin, collagen type I, osteopontin, and bone sialoprotein [22–24].

Methods of grafting of the RGD peptide onto the surface of implants are generally based on physical adhesion and chemical immobilization [25]. Physical adhesion is mainly related to the spontaneous adhesion of coating materials to the surface of an implant material. This method is effective for coating bioactive materials to the surface of implants but is limited in its application to a number of materials. On the contrary, chemical fixation has the advantage of forming firm and stable coating layers, although these methods comprise several complicated processes [4].

Most studies have focused on the attachment, proliferation, and osteogenic functionality of bone-forming cells. However, a few studies have been carried out to investigate the relationship between the RGD peptide and bone-resorbing cells such as osteoclasts [26, 27].

The purpose of this work was to (1) characterize RGD peptide immobilized on the surface of 30- and 100-nm TiO₂ nanotubes and (2) to examine the effects of RGD peptide-coated TiO₂ nanotubes on the cellular response and functionality of osteogenic-induced human mesenchymal stem cells (hMSCs), which are osteoclasts that have been induced by bone marrow macrophages.

2. Experimental Section

2.1. TiO₂ Nanotubes Fabrication. TiO₂ nanotube surfaces were prepared by previous reports [14], and the anodization process was carried out as follows. The bare Ti sheet (Hyundai Titanium Co., 0.2 mm thick, 99.5%, Republic of Korea) was cleaned with acetone and deionized water. TiO₂ nanotubes were prepared in 0.5 w/v% hydrofluoric acid (Merck, 48 w/v%, NJ, USA) in water with acetic acid (JT Baker, 98 w/v%,

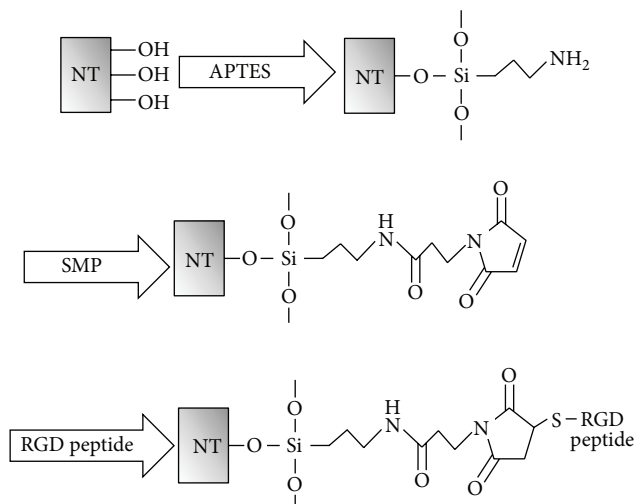


FIGURE 1: Reaction schematic diagram of TiO₂ nanotube surface modification procedure: (I) silane (APTES) treatment; (II) bifunctional cross-linker (SMP) connection; and (III) Arg-Gly-Asp (RGD) peptide grafting.

NJ, USA; volumetric ratio = 7:1) at 5, 10, 15, and 20 V for 1 h. A platinum electrode (DSM Co., 99.99%, South Korea) served as the counterpart. The samples were then rinsed with deionized water, dried at 60°C, and heat-treated at 500°C for 2 hrs to crystallize amorphous TiO₂ nanotubes into anatase structures. The morphology of TiO₂ nanotube arrays was observed by field emission scanning electron microscope (FE-SEM; S4800, Hitachi/Horiba Co., Japan).

2.2. RGD Peptide-Coating Process. RGD peptide was obtained from Sigma (A8052, MO, USA) in this research. The procedure of RGD peptide immobilization (see Figure 1) contains the grafting of a 3-aminopropyltriethoxysilane (APTES) onto the surface of TiO₂ nanotubes, and the substitution of the terminal amine to maleimide group reacted with thiol group of RGD peptide via a heterobifunctional cross-linker (3-succinimidyl-3-maleimido propionate: SMP, Sigma, MO, USA). The whole processes of silanization, substitution, and RGD peptide immobilization were listed in previous reports [23, 28]. Briefly, UV-sterilized TiO₂ nanotube samples (1.27 × 1.27 cm²) were silanized by immersing experimental samples in 10 mM APTES dissolved in hexane for 2 h. The silanized TiO₂ nanotubes were substituted for maleimide groups by using 2 mM bifunctional cross-linker SMP dissolved in DMF for 2 h. And then, thiolized RGD peptide dissolved in anhydrous DMF was immobilized on TiO₂ nanotubes by stirring for 2 h. Thiolized RGD peptides were prepared by previous research [29]. All experimental procedures were performed under Ar atmosphere.

2.3. Surface Analysis. To analyze the chemical composition change of TiO₂ nanotubes before and after RGD peptide immobilization, X-ray diffractometer (X'Pert PRO MRD,

PANalytical B.V., the Netherlands) with Ni-filtered Cu-K α ray, Fourier transform infrared spectroscopy (FT-IR; Nicolet, Thermo Co., WI, USA) and X-ray photoelectron spectroscopy (XPS, K-Alpha ESKA system; Thermo, USA) were carried out. In terms of XRD measurement, the glancing angle of the specimen was fixed at 5° against the incident beam enabling the detection of XRD patterns to be at the depth of less than 5 μ m from the top surface of the substrate.

2.4. hMSCs Cell Culture. We obtained human mesenchymal stem cells (hMSCs) from Lonza Corporation (Poietics hMSCs, Switzerland). Also, we used cell growth media composed of α -MEM (Invitrogen, CA, USA), 10% fetal bovine serum (FBS) (Invitrogen), and 1% penicillin-streptomycin (Invitrogen). The CO₂ incubator conditions of hMSCs were 37°C and 5% CO₂ atmosphere. The experiments of hMSCs were conducted with cultures at passage 4-5. After the confluence of hMSCs, they were seeded onto TiO₂ nanotube experimental substrate placed on a 12-well plate (cell density of 25,000 cells in each well) and were stored in a CO₂ incubator for a range of incubation times. Osteogenic induction media were prepared by adding 10 mM β -glycerol phosphate (Sigma Co., MO, USA), 150 μ g/mL ascorbic acid (Sigma), and 10 nM dexamethasone (Sigma) to cell growth media and was added to promote the osteogenic differentiation of hMSCs after 3 days of incubation. Osteogenic induction media were changed every 2-3 days.

2.5. Cell Adhesion and Proliferation Test. To estimate the degree of cell adhesion at the beginning of incubation time, fluorescein diacetate (FDA; Sigma, MO, USA) techniques was conducted to count viable hMSCs adhered to the experimental specimen. At 2, 24, and 48 hrs after plating, hMSCs on the substrates were rinsed with phosphate buffered saline solution (PBS) solution (Invitrogen, CA, USA) and were incubated with an FDA working solution (50 μ g FDA dissolved in 10 mL PBS solution) for 30 seconds and were then washed three times by PBS solution. The washed specimens were viewed under an inverted fluorescence microscope (CKX41, Olympus Co., Japan). We counted FDA-stained hMSCs adhered at all four corners of a specimen and at the center of the specimen.

MTT (3-(4,5-dimethylthiazol-2-yl)-2,5-diphenyltetrazolium bromide) assay was conducted to investigate the proliferation of hMSCs cultured on various experimental specimens. The samples were washed by PBS solution and were transferred to a new 12-well plate after the selected incubation periods. 1 mL of MTT dye agent (Sigma) was added to each well. After 3 hrs of incubation in 5% CO₂ incubator, 1 mL of isopropanol was added to each well, and the 12-well plate was then shaken for 30 minutes. The absorbance of each solution was measured at 570 nm by a microplate ELISA reader (Spectra Max 250, Thermo Electron Co., USA). The MTT value of each experimental group was relatively evaluated by that of uncoated 30 nm TiO₂ nanotubes.

2.6. Alkaline Phosphatase (ALP) Activity Test. To confirm the osteogenic differentiation and functionality of hMSCs,

alkaline phosphatase (ALP) activity test was used. After 2 weeks of incubation, the experimental samples were rinsed with PBS solution and lysed by using lysis buffer solution (25 mM Tris, pH 7.6, 150 mM NaCl, and 1% NP-40) and were stored in ice for 30 minutes. 50 μ L of cell lysate was used for ALP activity assay, and the rest of the cell lysate was used to measure the total protein content (Bradford Protein Assay Kit, Bio-Rad Laboratories, USA). 50 μ L of cell lysate was mixed with 200 μ L of para-nitrophenylphosphate (p-NPP, Sigma, MO, USA), and the mixed solution was stored at 37°C for 30 min to activate the reaction. After 30 minutes, 50 μ L of 3N NaOH (Sigma, MO, USA) was added to the mixed solution to stop the reaction. The absorbance of each solution was measured at 405 nm by a microplate ELISA reader (Spectra Max 250, Molecular Device, CA, USA). The level of activity was normalized with the amounts of total protein in the cell lysates (units/mg protein).

2.7. Motility Test of hMSCs. The motility of hMSCs cultured on 30 and 100 nm TiO₂ nanotubes was examined by modified FDA staining technique. Half of TiO₂ nanotubes samples was covered by cellophane tape. And then, hMSCs were seeded onto TiO₂ nanotube experimental substrate placed on a 12-well plate (cell density of 25,000 cells in each well) and were stored in a CO₂ incubator for 24 hrs. After 24 h of incubation, cellophane tape was removed, and hMSCs cultured on experimental samples were cultured for additional 24 h. After 48 hrs of incubations, live hMSCs were stained by FDA solution, and the motility images of live hMSCs cultured on TiO₂ nanotubes were obtained by inverted fluorescence microscope.

2.8. Mice and Reagents for Osteoclast Experiment. C57BL/6 mice were purchased from Orient Bio Inc. (SungNam, Republic of Korea), and were used to produce bone marrow-derived-macrophages (BMMs). All mice used in these experiments were 6–8 weeks old, and all experiments were approved by the Animal Studies Committee of Wonkwang University. All cell culture media and supplements were obtained from Thermo Scientific Corporation (IL, USA). Soluble recombinant mouse RANKL was purified from insect cells as described previously [30], and recombinant human M-CSF was a gift from Daved H. Fremont (Washington University, St. Louis, MO, USA).

2.9. Osteoclast Formation and Staining on Peptide-Coated TiO₂ Nanotube. Murine osteoclasts were prepared from bone marrow cells using the standard methods as previously described with minor modification [30]. In brief, bone marrow (BM) cells were obtained by flushing femur and tibia from C57BL/6 mice. For stromal cell-free bone marrow-derived macrophage (BMM) culture, bone marrow cells were cultured with M-CSF (50 ng/mL) for 3 day in α -MEM containing 10% FBS, and attached cells were used as osteoclast precursors, BMMs. BMMs (6 \times 10⁴ cell/wells in 24-well plates) were loaded onto control or peptide-coated TiO₂ nanotube pieces (1.27 cm \times 1.27 cm), having 30 nm and 100 nm diameters, and were subsequently differentiated into

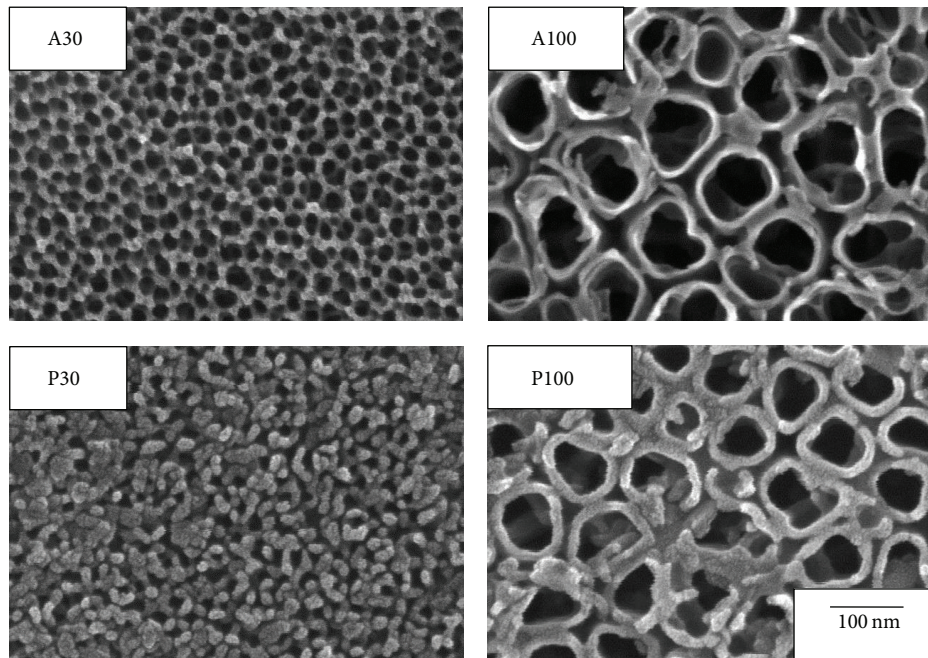


FIGURE 2: SEM micrographs of self-aligned 30 (A30), 100 (A100) nm TiO_2 nanotubes and RGD peptide-coated 30 (P30), 100 (P100) nm TiO_2 nanotubes. (The scale bar of all figures is 100 nm).

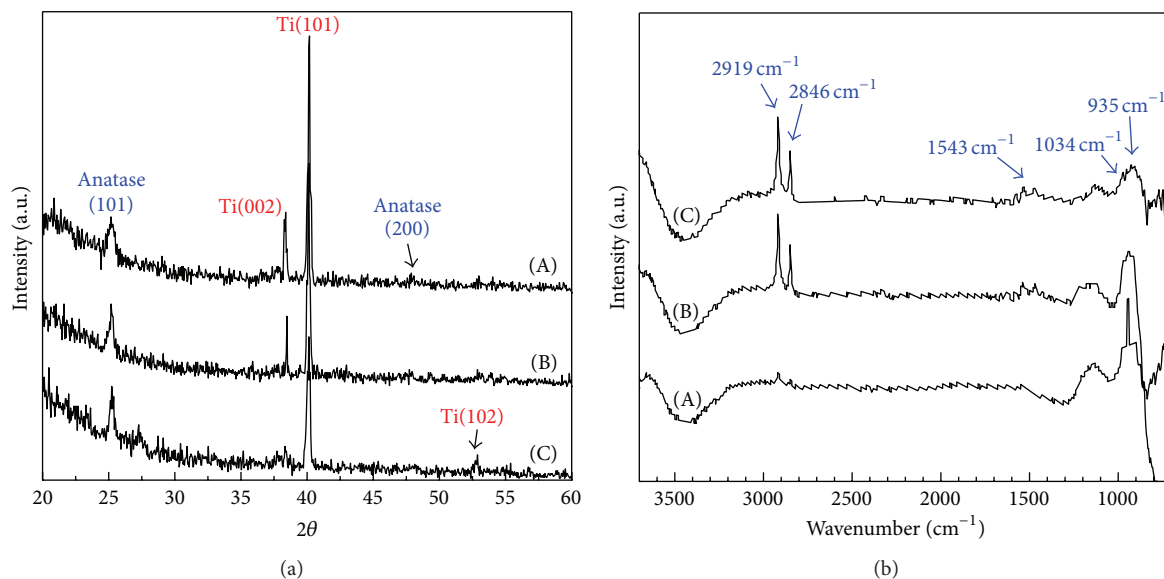
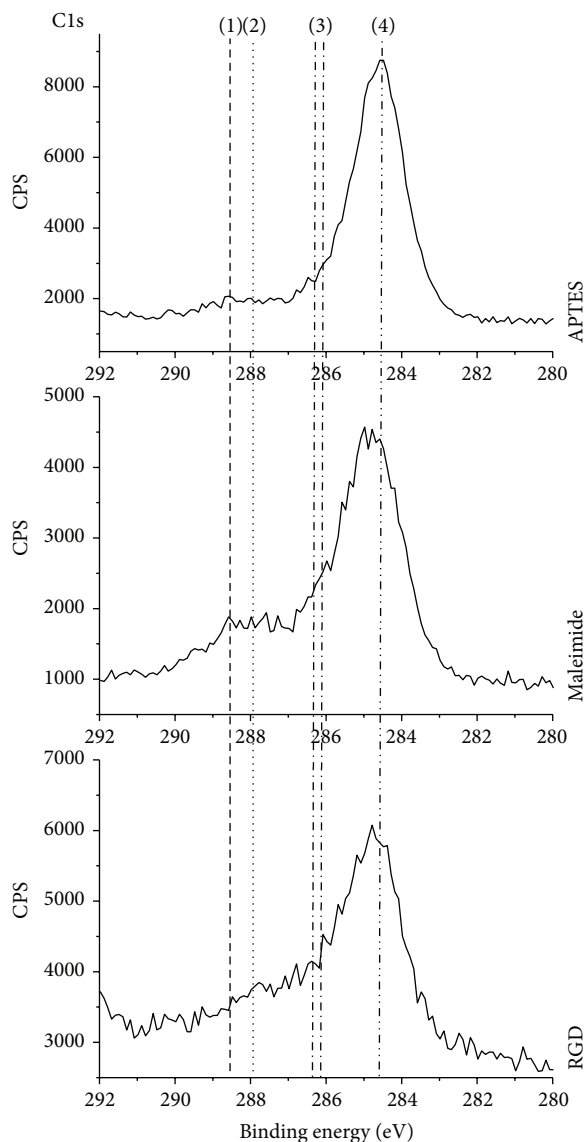


FIGURE 3: (a) XRD patterns and (b) FT-IR spectra of (A) uncoated, (B) silanized, and (C) RGD peptide-coated 100 nm TiO_2 nanotubes.

osteoclasts with M-CSF (50 ng/mL) and RANKL (100 ng/mL) for 4 day. Fresh media containing M-CSF and RANKL were resupplied at day 3. For coculture, bone marrow cells (6×10^5 cells/well) were cultured with calvaria-derived osteoblast (6×10^4 cells/well) on TiO_2 nanotubes. BM cells were differentiated into osteoclasts in α -MEM containing 10% FBS and were supplemented with $1\alpha,25(\text{OH})_2\text{D}_3$ (2×10^{-8} M) for 7 day. Cells were then stained with fluorescein diacetate (FDA; Sigma, MO, USA) as reported previously [31] and were pictured by an inverted fluorescence microscope (DM

IL LED, Leica Microsystems GmbH, Wetzlar, Germany). We tested osteoclast formation on TiO_2 nanotubes by three times and counted the number of mature osteoclast having characteristic actin ring. The representative data were shown.

2.10. Data Analysis. All data were expressed as mean \pm standard deviation and were statistically analyzed by one-way ANOVA (SPSS 12.0, SPSS GmbH, Germany) and the Student-Newman-Keuls method as a post hoc test. Significant differences were determined at P values at least less than 0.05.



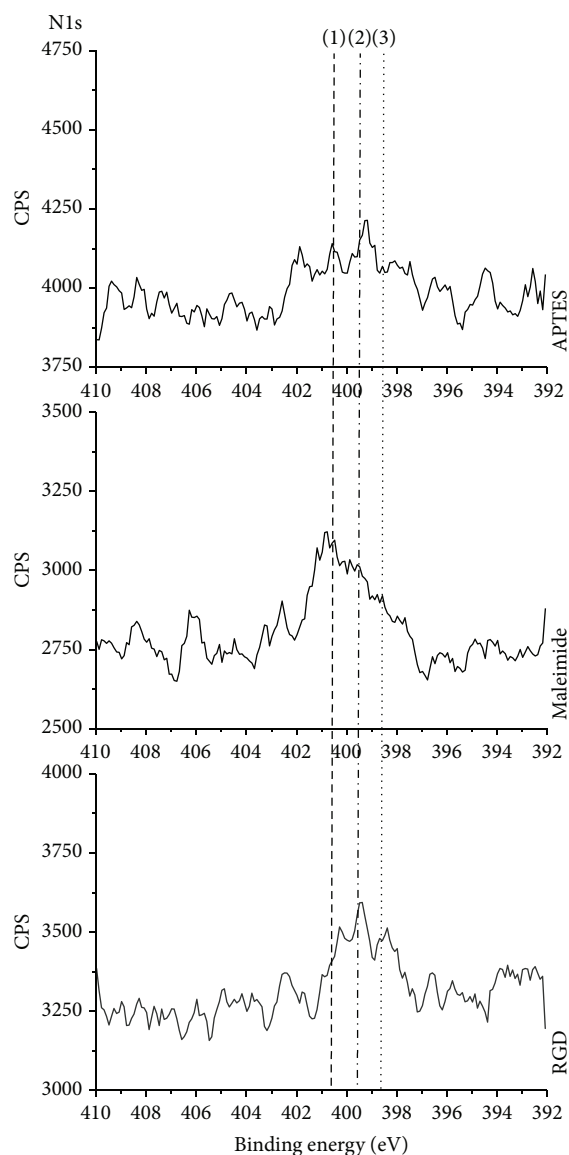
The list of related peak position

- (1) O=C-O (289 eV)
- (2) C=O, (288.3 eV)
- (3) N-C=O (286.4 eV), and C-NH₂, C-O (285.9–286.1 eV)
- (4) CHx or C-C (284.8 eV)

FIGURE 4: XPS C1s spectra of silanized (APTES), bifunctional cross-linked (maleimide), and (c) RGD peptide-coated 100 nm TiO₂ nanotubes.

3. Results and Discussion

3.1. Analysis of RGD Peptide Grafted onto TiO₂ Nanotubes. Figure 2 shows SEM micrographs of uncoated and RGD peptide-coated 30 and 100 nm TiO₂ nanotubes. As shown in the P30 and P100 images of Figure 2, 10–20 nm nanoparticles were deposited on the top surfaces of the TiO₂ nanotubes. We also tried to coat the RGD peptide onto TiO₂ nanotubes using 20 mM APTES and found that APTES coated the TiO₂ nanotubes completely, thereby blocking the pores (data not



The list of related peak position

- (1) Maleimide (399.7–400.7 eV)
- (2) N-C=O (399.7–400.8 eV)
- (3) C-NH₂, C-O (398.9 eV)

FIGURE 5: XPS N1s spectra of silanized (APTES), bifunctional cross-linked (maleimide), and (c) RGD peptide-coated 100 nm TiO₂ nanotubes.

shown). Therefore, we expect that 10 mM APTES is suitable for coating the RGD peptide onto the top surfaces of TiO₂ nanotubes effectively.

Figure 3 indicates the XRD patterns of FT-IR spectra of uncoated, silanized, and RGD peptide-coated 100-nm TiO₂ nanotubes, respectively. As shown by the XRD patterns, the crystal structures of the TiO₂ nanotubes prepared in this study were anatase. In the FT-IR spectra, some new peaks corresponding to the covalent grafting of APTES were detected at 935 (Si-OH), 1034 (Si-O-Si), 1543, 2846,

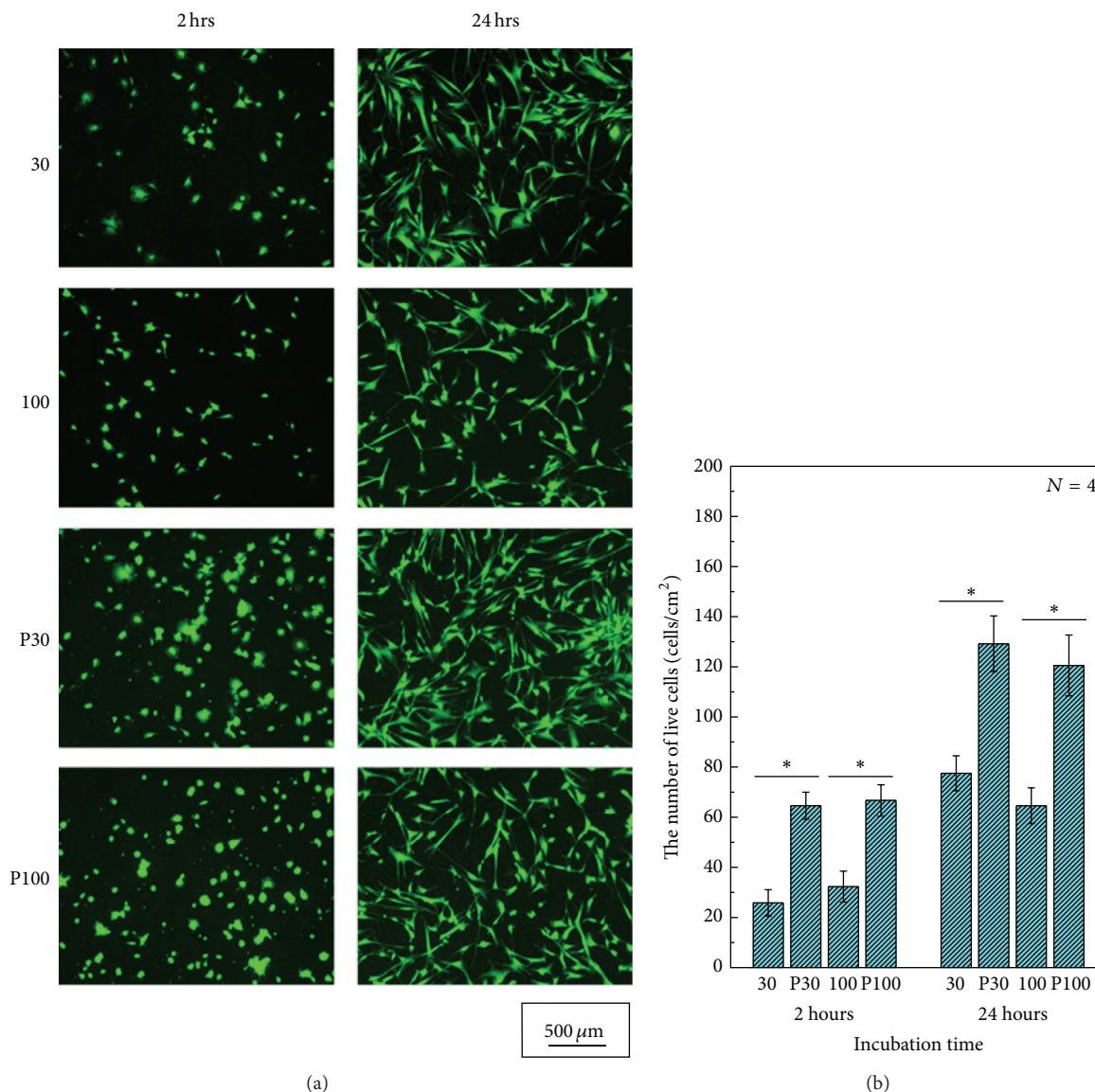


FIGURE 6: (a) Fluorescein diacetate (FDA) images and (b) the number of live hMSCs cultured on uncoated and RGD peptide-coated 30 and 100 nm TiO_2 nanotubes.

and 2919 cm^{-1} for the FT-IR spectra of the silanized and RGD peptide-coated TiO_2 nanotubes [32, 33]. As previously reported, these peaks originated from the formation of $\text{SiO}_{3/2}$ (silsequioxane) nanoparticles [34]. From the results of FT-IR analysis of the RGD peptide, it was difficult to identify the existence of RGD peptides immobilized on TiO_2 nanotubes because of the overlap of the FT-IR spectral peaks between APTES and the RGD peptide. Therefore, XPS analysis was used to confirm the covalent grafting of the RGD peptide onto the TiO_2 nanotube surface.

Figures 4 and 5 show the XPS spectra of Cls and N1s for silanized (APTES), bifunctional cross-linked (maleimide), and the RGD peptide-coated TiO_2 nanotube substrates, respectively. Four kinds of Cls peaks were detected on the surfaces of the APTES, maleimide, and RGD peptide-coated

TiO_2 nanotubes as shown in Figure 4. From the 4 kinds of Cls peaks, lines 1 and 2 (binding energies of 289 and 288.3) indicate the portions of $\text{O}=\text{C}-\text{O}$ and $\text{C}=\text{O}$ derived from maleimide and RGD peptide, respectively. Line 3 (binding energy of 285.9–286.4 eV) indicates the existence of the RGD peptide. Line 4 (binding energy of 284.8 eV) represents the silanization by APTES [35]. As seen in Figure 5, the 3 kinds of N1s peaks were detected on the surface of APTES, maleimide, and the RGD peptide-coated TiO_2 nanotubes. Line 1 and 2 show the overlap of maleimide and the RGD peptide. However, line 3 indicates the portions of $\text{C}-\text{NH}_3$ and $\text{C}-\text{O}$ bonds that originated from the RGD peptide [36, 37].

From the SEM observations and the results of FT-IR analysis, it was confirmed that 10–20 nm $\text{SiO}_{3/2}$ nanoparticles were deposited on the surfaces of the TiO_2 nanotubes. In

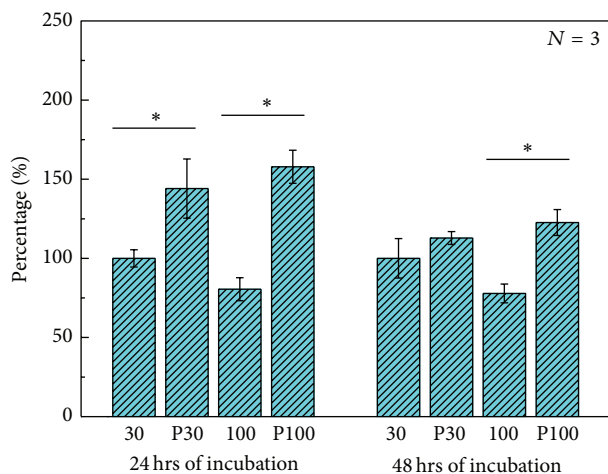


FIGURE 7: The result of the MTT with hMSCs cultured on uncoated and RGD peptide-coated 30 and 100 nm TiO₂ nanotubes after 24 h and 48 hrs of incubation. * denotes significance between uncoated and RGD peptide-coated TiO₂ nanotubes.

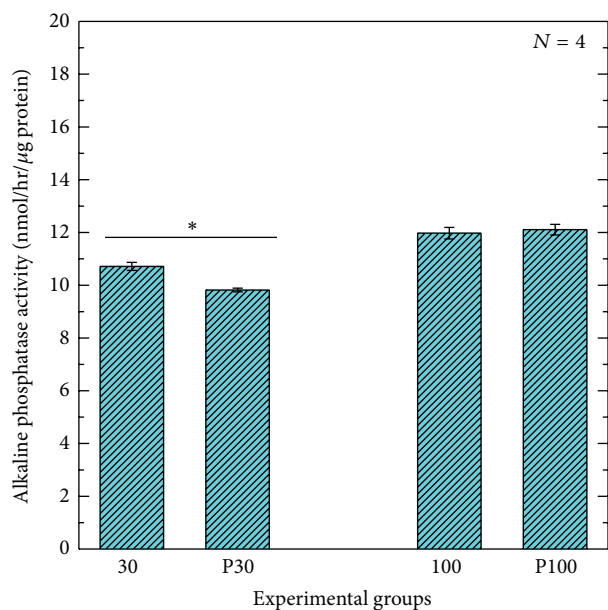


FIGURE 8: Alkaline phosphatase (ALP) activity of hMSCs cultured on uncoated and RGD peptide-coated 30 and 100 nm TiO₂ nanotubes after 2 weeks of incubation. * denotes significance between uncoated 30 nm TiO₂ nanotubes versus RGD peptide-coated 30 nm TiO₂ nanotubes.

addition, the XPS analysis indicated that the RGD peptide was coated onto the surface of TiO₂ nanotubes through silanization and bifunctional cross-linking.

3.2. Initial Attachment and Proliferation of hMSCs. Figure 6 shows images of FDA stained, live hMSCs cultured on uncoated and RGD peptide-coated 30 and 100 nm TiO₂ nanotubes after 2 and 24 hours of incubation. As shown

in Figure 6(b), after 2 and 24 hours of incubation, the number of hMSCs that were cultured on the RGD peptide-coated TiO₂ nanotubes was significantly higher than that on uncoated TiO₂ nanotubes, regardless of the diameter of the TiO₂ nanotubes ($P < 0.05$). Thus, it was confirmed that the RGD peptide-coating enhanced the initial attachment of hMSCs to the surface of TiO₂ nanotubes within 24 h of incubation.

Figure 7 shows the MTT assay results for uncoated and RGD peptide-coated 30 and 100 nm TiO₂ nanotubes after 24 and 48 h of incubation. The values for the RGD peptide-coated TiO₂ nanotubes were significantly higher than those for the uncoated TiO₂ nanotubes ($P < 0.05$). However, no significant difference was observed between the uncoated and RGD peptide-coated 30 nm TiO₂ nanotubes after 48 h of incubation ($P > 0.05$). Previous reports have shown that the initial attachment and proliferation of cells cultured on 30 nm TiO₂ nanotubes are higher than those on 100 nm TiO₂ nanotubes at the beginning of incubation time [15, 38]. Therefore, 48 h of incubation may have been long enough to overcome RGD peptide feature promoting the initial cell attachment when it was coated onto the surface of 30 nm TiO₂ nanotubes. Thus, the MTT assay results for the uncoated and RGD peptide-coated 30 nm TiO₂ nanotubes after 48 h of incubation can be considered similar.

From the results of FDA staining and the MTT assay, we confirmed that the RGD peptide promoted the attachment and proliferation of hMSCs cultured on TiO₂ nanotubes at the beginning of incubation.

3.3. ALP Activity of hMSCs. Figure 8 shows the results of the ALP activity assay of hMSCs cultured on uncoated and RGD peptide-coated 30 and 100 nm TiO₂ nanotubes after 2 weeks of incubation. The ALP activity of the hMSCs cultured on RGD peptide-coated 30 nm TiO₂ nanotubes was significantly lower than that of hMSCs cultured on uncoated 30 nm TiO₂ nanotubes ($P < 0.05$). In addition, no significant difference was observed in the ALP activity between uncoated and the RGD peptide-coated 100 nm TiO₂ nanotubes ($P > 0.05$).

Although the results of FDA staining and the MTT assay were similar to those obtained in previous studies [39], the results of the ALP activity assay were not as consistent. The bond status of the RGD peptide, nature of the biomaterials, and cell culture periods play important roles during initial attachment, in osteogenic differentiation and in the functionality of mesenchymal stem cells [40–43]. In this study, we prepared thiolized RGD peptide instead of purchasing cysteine-conjugated RGD peptide, which was used in previous studies [23, 28, 39]. Therefore, the bond status of the functional groups between the thiolized RGD peptide and the cysteine-conjugated RGD peptide can be safely assumed to be different, which makes the results, in terms of cellular response, obtained using these 2 peptides different. Furthermore, many published studies on the effects of the RGD peptide on cellular responses have focused on ceramic surfaces instead of metal surfaces, which would result in discrepancies in the results in terms of cellular proliferation and differentiation [44–47].

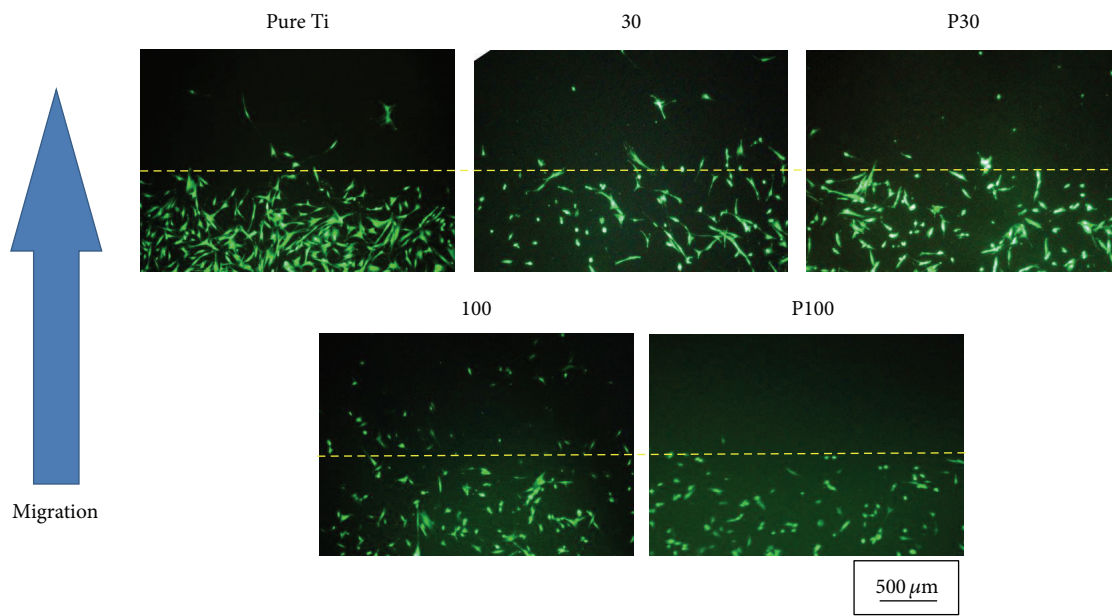


FIGURE 9: Fluorescein diacetate (FDA) images of live hMSCs cultured on pure Ti, uncoated, and RGD peptide-coated 30 and 100 nm TiO_2 nanotube after 48 hours of incubation. (Motility test of hMSCs). # Upper half area is covered by cellophane tape when hMSCs are seeded onto substrate. After 24 h of incubation, cellophane tape was removed, and then hMSCs was cultured for addition 24 h.

In addition, the motility and mechanical strain of hMSCs cultured on biomaterials promote the osteogenic differentiation of hMSCs [48, 49]. To prove the correlation between cell motility and osteogenic differentiation, the motility of the hMSCs during 24 hours of incubation was examined using through FDA staining. As shown in Figure 9, the motility of the hMSCs cultured on uncoated TiO_2 nanotubes seemed to be higher than that of hMSCs cultured on RGD peptide-coated TiO_2 nanotubes. Therefore, we believe that the RGD peptide that coated the surfaces of the TiO_2 nanotubes suppressed hMSC motility. We also think that the results of the ALP activity assay were affected by the properties of the RGD peptide, nature of the biomaterial surface, and motility of cells that are cultured on variously sized TiO_2 nanotubes. Further investigation is performed to resolve the inconsistency between MTT and ALP activity results more clearly.

3.4. Attachment and Proliferation of BMM and Maturation of Osteoclasts. *In vivo*, osteoblasts, which are bone-forming cells, reside with osteoclasts, which are bone-resorbing cells, within the same compartment. Therefore, examining the effect of RGD peptide-coated TiO_2 nanotubes on osteoclast formation, together with their effect on osteoblasts, is important. We cultured osteoclasts on RGD peptide-coated TiO_2 nanotubes and assessed the effect of the RGD peptide-coating on the formation of mature osteoclast. Previously, we reported that the adhesion ability of osteoclast precursors attached to TiO_2 nanotubes of various pore diameters (30–100 nm) was not different. However, osteoclast formation decreased with increasing nanotube diameter [50]. Consistent with our previous data, Figure 10 shows that the formation of mature osteoclasts on uncoated 100 nm TiO_2

nanotubes was significantly less than that on uncoated 30 nm TiO_2 nanotubes in both culture systems (BMM culture and coculture). Although mature osteoclast formation on the RGD peptide-coated 30-nm TiO_2 nanotubes was diminished slightly than uncoated 30 nm TiO_2 nanotubes, however, mature osteoclast formation was highly maintained on RGD peptide-coated 30 nm TiO_2 in the BMM culture (Figure 10(a)). Moreover, mature osteoclast formation was dramatically increased on the RGD peptide-coated 100 nm TiO_2 nanotubes compared to that of uncoated 100 nm TiO_2 nanotubes which inhibited mature osteoclast formation (Figure 10(a)). In addition, mature osteoclast formation on the RGD peptide-coated 100 nm TiO_2 nanotubes also increased significantly to the same level as that of the RGD peptide-coated or uncoated 30 nm TiO_2 nanotubes in the coculture system (Figure 10(b)). These data suggest that the RGD peptide-coated onto the TiO_2 nanotubes promoted the initial attachment of osteoclasts [51, 52] and that it helped overcome the inhibitory effect of nanotubes with large pores on osteoclast formation. As mentioned above, cell attachment and functionality depend on many factors such as cell phenotype, shape, culture media, and the surface used for cell culture. However, in this study, the RGD peptide seemed to enhance the initial attachment and proliferation of hMSCs and BMMs, and the maturation of preosteoclasts into bone-resorbing mature osteoclasts.

4. Conclusions

In this study, the RGD peptide was grafted covalently onto the surface of TiO_2 nanotubes based on the results of SEM analysis, FT-IR, and XPS. Furthermore, the RGD peptide promoted the initial attachment and proliferation of hMSCs,

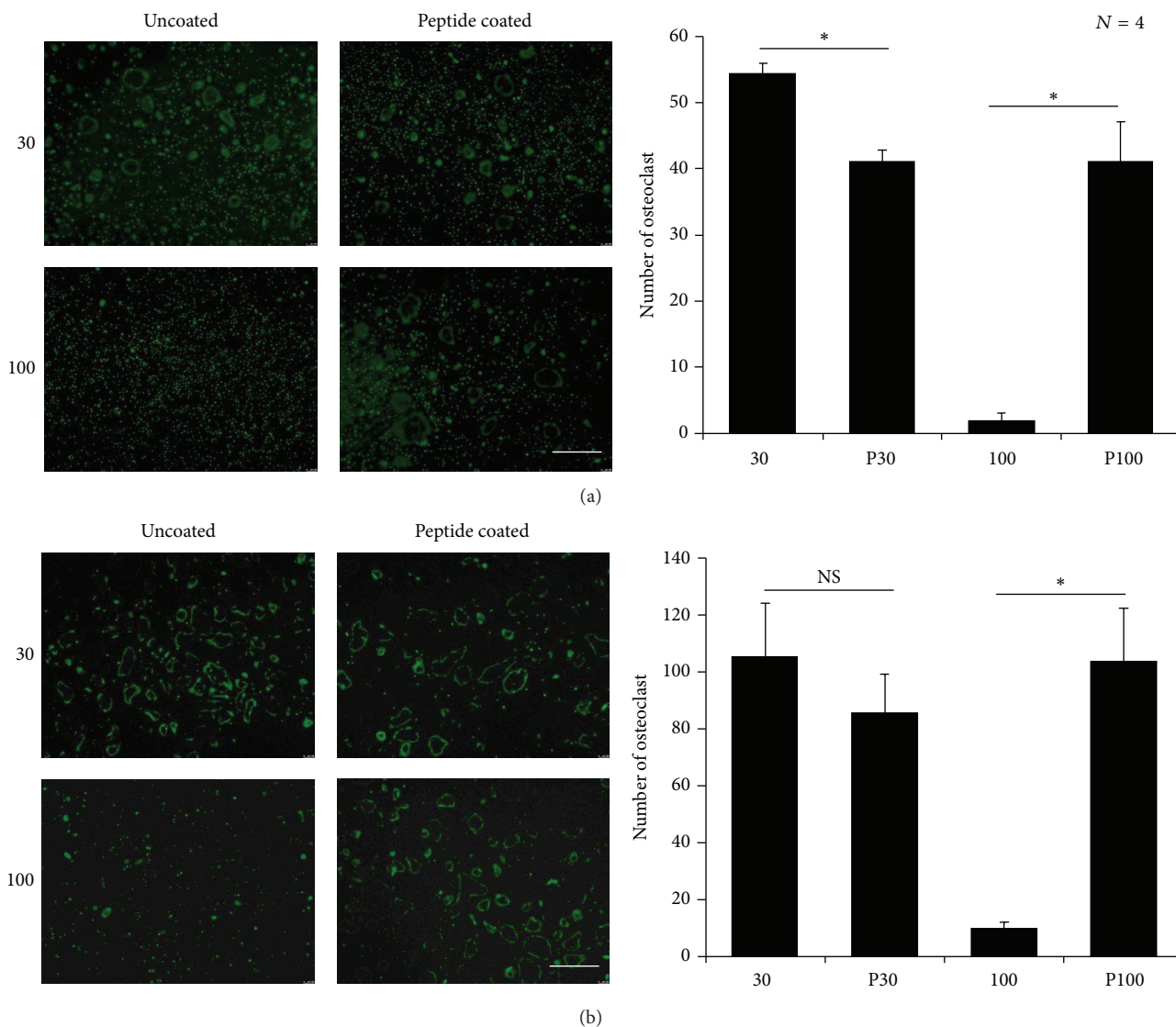


FIGURE 10: Bone marrow derived-macrophages under M-CSF and RANKL treatment were cultured, (a) and bone marrow cells under $\alpha,25(\text{OH})_2\text{D}_3$ treatment were cocultured with osteoblast (b) on uncoated (30 and 100) and RGD peptide- (P30 and P100) coated TiO₂ nanotubes. Cells were then stained with fluorescein diacetate (FDA). Cells having actin ring were counted as mature osteoclast. Bar = 500 μm .

regardless of the size of the TiO₂ nanotube. However, the RGD peptide did not prominently affect the osteogenic functionality of the hMSCs because the peptide suppressed the motility of the hMSCs during osteogenic differentiation. The result of the osteoclast *in vitro* test showed that the RGD peptide accelerated the initial attachment of preosteoclasts and the formation of mature osteoclasts, which can resorb the bone matrix. Therefore, we believe that applying an RGD coating onto TiO₂ nanotubes synthesized on Ti implants that are used in medicine might not accelerate bone formation *in vivo* significantly because osteoblasts and osteoclasts reside in the same compartment.

Acknowledgment

This paper was supported by Wonkwang University in 2011.

References

- [1] L. Le Guéhennec, A. Soueidan, P. Layrolle, and Y. Amouriq, "Surface treatments of titanium dental implants for rapid osseointegration," *Dental Materials*, vol. 23, no. 7, pp. 844–854, 2007.
- [2] R. Junker, A. Dimakis, M. Thoneick, and J. A. Jansen, "Effects of implant surface coatings and composition on bone integration: a systematic review," *Clinical Oral Implants Research*, vol. 20, no. 4, pp. 185–206, 2009.
- [3] D. A. Puleo and A. Nanci, "Understanding and controlling the bone-implant interface," *Biomaterials*, vol. 20, no. 23-24, pp. 2311–2321, 1999.
- [4] M. Dettin, M. T. Conconi, R. Gambaretto et al., "Effect of synthetic peptides on osteoblast adhesion," *Biomaterials*, vol. 26, no. 22, pp. 4507–4515, 2005.
- [5] Y. Kataoka, Y. Tamaki, and T. Miyazaki, "Synergistic responses of superficial chemistry and micro topography of titanium

- created by wire-type electric discharge machining,” *Bio-medical Materials and Engineering*, vol. 21, no. 2, pp. 113–121, 2011.
- [6] K. Kim, T. Kwon, S. Kim et al., “Preparation and characterization of anodized titanium surfaces and their effect on osteoblast responses,” *The Journal of Oral Implantology*, vol. 32, no. 1, pp. 8–13, 2006.
 - [7] G. Balasundaram, C. Yao, and T. J. Webster, “TiO₂ nanotubes functionalized with regions of bone morphogenetic protein-2 increases osteoblast adhesion,” *Journal of Biomedical Materials Research A*, vol. 84, no. 2, pp. 447–453, 2008.
 - [8] M. Sato and T. J. Webster, “Nanobiotechnology: implications for the future of nanotechnology in orthopedic applications,” *Expert Review of Medical Devices*, vol. 1, no. 1, pp. 105–114, 2004.
 - [9] K. S. Brammer, S. Oh, J. O. Gallagher, and S. Jin, “Enhanced cellular mobility guided by TiO₂ nanotube surfaces,” *Nano Letters*, vol. 8, no. 3, pp. 786–793, 2008.
 - [10] M. J. Dalby, L. Di Silvio, E. J. Harper, and W. Bonfield, “Initial interaction of osteoblasts with the surface of a hydroxyapatite-poly(methylmethacrylate) cement,” *Biomaterials*, vol. 22, no. 13, pp. 1739–1747, 2001.
 - [11] M. J. Dalby, N. Gadegaard, P. Herzyk et al., “Nanomechanotransduction and interphase nuclear organization influence on genomic control,” *Journal of Cellular Biochemistry*, vol. 102, no. 5, pp. 1234–1244, 2007.
 - [12] M. J. Dalby, “Nanostructured surfaces: cell engineering and cell biology,” *Nanomedicine*, vol. 4, no. 3, pp. 247–248, 2009.
 - [13] J. O. Gallagher, K. F. McGhee, C. D. W. Wilkinson, and M. O. Riehle, “Interaction of animal cells with ordered nanotopography,” *IEEE Transactions on Nanobioscience*, vol. 1, no. 1, pp. 24–28, 2002.
 - [14] S. Oh, C. Daraio, L. Chen, T. R. Pisanic, R. R. Fiñones, and S. Jin, “Significantly accelerated osteoblast cell growth on aligned TiO₂ nanotubes,” *Journal of Biomedical Materials Research A*, vol. 78, no. 1, pp. 97–103, 2006.
 - [15] J. Park, S. Bauer, K. Von Der Mark, and P. Schmuki, “Nanosize and vitality: TiO₂ nanotube diameter directs cell fate,” *Nano Letters*, vol. 7, no. 6, pp. 1686–1691, 2007.
 - [16] L. M. Bjursten, L. Rasmusson, S. Oh, G. C. Smith, K. S. Brammer, and S. Jin, “Titanium dioxide nanotubes enhance bone bonding in vivo,” *Journal of Biomedical Materials Research A*, vol. 92, no. 3, pp. 1218–1224, 2010.
 - [17] L. Meirelles, L. Melin, T. Peltola et al., “Effect of hydroxyapatite and titania nanostructures on early in vivo bone response,” *Clinical Implant Dentistry and Related Research*, vol. 10, no. 4, pp. 245–254, 2008.
 - [18] G. Giavaresi, M. Tschon, J. H. Daly et al., “In vitro and in vivo response to nanotopographically-modified surfaces of poly(3-hydroxybutyrate-co-3-hydroxyvalerate) and polycaprolactone,” *Journal of Biomaterials Science*, vol. 17, no. 12, pp. 1405–1423, 2006.
 - [19] K. Huo, X. Zhang, H. Wang, L. Zhao, X. Liu, and P. K. Chu, “Osteogenic activity and antibacterial effects on titanium surfaces modified with Zn-incorporated nanotube arrays,” *Biomaterials*, vol. 34, no. 13, pp. 3467–3478, 2013.
 - [20] T. Albrektsson and C. Johansson, “Osteoinduction, osteoconduction and osseointegration,” *European Spine Journal*, vol. 10, no. 2, pp. S96–S101, 2001.
 - [21] M. Dard, A. Sewing, J. Meyer, S. Verrier, S. Roessler, and D. Scharnweber, “Tools for tissue engineering of mineralized oral structures,” *Clinical oral investigations*, vol. 4, no. 2, pp. 126–129, 2000.
 - [22] E. Ruoslahti and M. D. Pierschbacher, “Arg-Gly-Asp: a versatile cell recognition signal,” *Cell*, vol. 44, no. 4, pp. 517–518, 1986.
 - [23] S. Xiao, M. Textor, N. D. Spencer, and H. Sigrist, “Covalent attachment of cell-adhesive, (Arg-Gly-Asp)-containing peptides to titanium surfaces,” *Langmuir*, vol. 14, no. 19, pp. 5507–5516, 1998.
 - [24] S. P. Massia and J. A. Hubbell, “Covalently attached GRGD on polymer surfaces promotes biospecific adhesion of mammalian cells,” *Annals of the New York Academy of Sciences*, vol. 589, pp. 261–270, 1990.
 - [25] A. Rezanian, R. Johnson, A. R. Lefkowitz, and K. E. Healy, “Bioactivation of metal oxide surfaces. 1. Surface characterization and cell response,” *Langmuir*, vol. 15, no. 20, pp. 6931–6939, 1999.
 - [26] K. Yip and D. J. Marsh, “An Arg-Gly-Asp peptide stimulates constriction in rat afferent arteriole,” *American Journal of Physiology*, vol. 273, no. 5, pp. F768–F776, 1997.
 - [27] J. Reed, W. E. Hull, C.-W. Von Der Lieth, D. Kubler, S. Suhai, and V. Kinzel, “Secondary structure of the Arg-Gly-Asp recognition site in proteins involved in cell-surface adhesion. Evidence for the occurrence of nested β -bends in the model hexapeptide GRGDSP,” *European Journal of Biochemistry*, vol. 178, no. 1, pp. 141–154, 1988.
 - [28] M. C. Durrieu, S. Pallu, F. Guillemot et al., “Grafting RGD containing peptides onto hydroxyapatite to promote osteoblastic cells adhesion,” *Journal of Materials Science*, vol. 15, no. 7, pp. 779–786, 2004.
 - [29] J. Carter, “Conjugation of peptide to carrier proteins via m-Maleimidobenzoyl-N-Hydroxysuccinimide ester (MBS),” in *The Protein Protocols Handbook*, pp. 689–692, 1996.
 - [30] S. H. Lee, T. Kim, D. Jeong, N. Kim, and Y. Choi, “The Tec family tyrosine kinase Btk regulates RANKL-induced osteoclast maturation,” *The Journal of Biological Chemistry*, vol. 283, no. 17, pp. 11526–11534, 2008.
 - [31] K. Moon, S. Yu, J. Bae, and S. Oh, “Biphasic osteogenic characteristics of human mesenchymal stem cells cultured on TiO₂ nanotubes of different diameters,” *Journal of Nanomaterials*, vol. 2012, Article ID 252481, 8 pages, 2012.
 - [32] Y. Zhang, Y. Yuan, and C. Liu, “Fluorescent labeling of nanometer hydroxyapatite,” *Journal of Materials Science and Technology*, vol. 24, no. 2, pp. 187–191, 2008.
 - [33] E. T. Vandenberg, L. Bertilsson, B. Liedberg et al., “Structure of 3-aminopropyl triethoxy silane on silicon oxide,” *Journal of Colloid And Interface Science*, vol. 147, no. 1, pp. 103–118, 1991.
 - [34] G. Lu, Y. Huang, Y. Yan, T. Zhao, and Y. Yu, “Synthesis and properties of bismaleimide-modified novolak resin/silsesquioxane nanocomposites,” *Journal of Polymer Science A*, vol. 41, no. 16, pp. 2599–2606, 2003.
 - [35] M. C. Durrieu, S. Pallu, F. Guillemot et al., “Grafting RGD containing peptides onto hydroxyapatite to promote osteoblastic cells adhesion,” *Journal of Materials Science*, vol. 15, no. 7, pp. 779–786, 2004.
 - [36] J. Charlier, V. Detalle, F. Valin, C. Bureau, and G. Lécayon, “Study of ultrathin polyamide-6,6 films on clean copper and platinum,” *Journal of Vacuum Science and Technology A*, vol. 15, no. 2, pp. 353–364, 1997.
 - [37] L. N. Bui, M. Thompson, N. B. McKeown, A. D. Romaschin, and P. G. Kalman, “Surface modification of the biomedical polymer poly(ethylene terephthalate),” *The Analyst*, vol. 118, no. 5, pp. 463–474, 1993.
 - [38] S. Oh, K. S. Brammer, Y. S. J. Li et al., “Stem cell fate dictated solely by altered nanotube dimension,” *Proceedings of*

- the National Academy of Sciences of the United States of America*, vol. 106, no. 7, pp. 2130–2135, 2009.
- [39] X. Cao, W. Yu, J. Qiu, Y. Zhao, Y. Zhang, and F. Zhang, “RGD peptide immobilized on TiO₂ nanotubes for increased bone marrow stromal cells adhesion and osteogenic gene expression,” *Journal of Materials Science*, vol. 23, pp. 527–536, 2012.
- [40] E. Ruoslahti, “RGD and other recognition sequences for integrins,” *Annual Review of Cell and Developmental Biology*, vol. 12, pp. 697–715, 1996.
- [41] Z. Qu, J. Yan, B. Li, J. Zhuang, and Y. Huang, “Improving bone marrow stromal cell attachment on chitosan/hydroxyapatite scaffolds by an immobilized RGD peptide,” *Biomedical Materials*, vol. 5, no. 6, Article ID 065001, 2010.
- [42] Y. Huang, J. Ren, T. Ren et al., “Bone marrow stromal cells cultured on poly (lactide-co-glycolide)/nano- hydroxyapatite composites with chemical immobilization of Arg-Gly-Asp peptide and preliminary bone regeneration of mandibular defect thereof,” *Journal of Biomedical Materials Research A*, vol. 95, no. 4, pp. 993–1003, 2010.
- [43] C. Yang, K. Cheng, W. Weng, and C. Yang, “Immobilization of RGD peptide on HA coating through a chemical bonding approach,” *Journal of Materials Science*, vol. 20, no. 11, pp. 2349–2352, 2009.
- [44] M. Jager, C. Boge, R. Janissen et al., “Osteoblastic potency of bone marrow cells cultivated on functionalized biomaterials with cyclic RGD-peptide,” *Journal of Biomedical Materials Research A*, 2013.
- [45] D. Le Guillou-Buffello, R. Bareille, M. Gindre, A. Sewing, P. Laugier, and J. Amédée, “Additive effect of RGD coating to functionalized titanium surfaces on human osteoprogenitor cell adhesion and spreading,” *Tissue Engineering A*, vol. 14, no. 8, pp. 1445–1455, 2008.
- [46] S. Tosatti, Z. Schwartz, C. Campbell et al., “RGD-containing peptide GCRGYGRGDSPG reduces enhancement of osteoblast differentiation by poly(L-lysine)-graft-poly(ethylene glycol)-coated titanium surfaces,” *Journal of Biomedical Materials Research - Part A*, vol. 68, no. 3, pp. 458–472, 2004.
- [47] S. Pallu, C. Bourget, R. Bareille et al., “The effect of cyclo-DfKRG peptide immobilization on titanium on the adhesion and differentiation of human osteoprogenitor cells,” *Biomaterials*, vol. 26, no. 34, pp. 6932–6940, 2005.
- [48] T. Briggs, M. D. Treiser, P. F. Holmes, J. Kohn, P. V. Moghe, and T. L. Arinzeh, “Osteogenic differentiation of human mesenchymal stem cells on poly(ethylene glycol)-variant biomaterials,” *Journal of Biomedical Materials Research A*, vol. 91, no. 4, pp. 975–984, 2009.
- [49] R. D. Sumanasinghe, S. H. Bernacki, and E. G. Lobo, “Osteogenic differentiation of human mesenchymal stem cells in collagen matrices: effect of uniaxial cyclic tensile strain on bone morphogenetic protein (BMP-2) mRNA expression,” *Tissue Engineering*, vol. 12, no. 12, pp. 3459–3465, 2006.
- [50] S. Oh and S. H. Lee, “Ability of osteoclasts adhesion and differentiation on various pore scale of TiO₂ nanotube surface,” *The Journal of the Korea Society For Dental Research Materials*, vol. 36, no. 4, pp. 315–320, 2009.
- [51] P. T. Lakkakorpi, G. Wesolowski, Z. Zimolo, G. A. Rodan, and S. B. Rodan, “Phosphatidylinositol 3-kinase association with the osteoclast cytoskeleton, and its involvement in osteoclast attachment and spreading,” *Experimental Cell Research*, vol. 237, no. 2, pp. 296–306, 1997.
- [52] B. Christensen, C. C. Kazanecki, T. E. Petersen, S. R. Rittling, D. T. Denhardt, and E. S. Sørensen, “Cell type-specific post-translational modifications of mouse osteopontin are associated with different adhesive properties,” *The Journal of Biological Chemistry*, vol. 282, no. 27, pp. 19463–19472, 2007.



Hindawi

Submit your manuscripts at
<http://www.hindawi.com>

